PCCP

Accepted Manuscript

ROYAL SOCIETY OF CHEMISTRY

www.rsc.org/pccp

Probing Surface States in PbS Nanocrystal Films Using Pentacene Field Effect Transistors: Controlling Carrier Concentration and Charge Transport in Pentacene.

Byoungnam Park[*,1,†, ‡], *Kevin Whitham*[2,‡], *Kaifu Bian*[1], *Yee-Fun Lim*[3], *and Tobias Hanrath*[1,*]

[1]School of Chemical and Biomolecular Engineering, [2]Department of Materials Science and Engineering, and [3]Department of Applied and Engineering Physics, Cornell University, Ithaca, New York 14853. ‡These authors contributed equally

KEYWORDS Nanoparticle, organic electronics, charge trapping, field effect transistors

ABSTRACT

We used a bilayer field effect transistor (FET) consisting of a thin PbS nanocrystals (NCs) film interfaced with vacuum-deposited pentacene to probe trap states in NCs. We interpret the observed threshold voltage shift in context of charge carrier trapping by PbS NCs and relate the magnitude of the threshold voltage shift to the number of trapped carriers. We explored a series of NC surface ligands to modify the interface between PbS NCs and pentacene and demonstrate the impact of interface chemistry on charge carrier density and the FET mobility in a pentacene FET.

Colloidal nanocrystals (NCs) are attractive building blocks for optoelectronic applications by virtue of their unique size-tunable optical and electrical properties. The ability to tailor properties by adjusting NC size, shape and composition has created new opportunities for emerging low cost, thin film nanotechnologies. Lead chalcogenide (PbX, X=S,Se,Te) NCs in particular have garnered immense interest and have played a leading role in enabling an impressive range of prototype PV[1-9] and LED[10] technologies. Integration of inorganic NCs with organic materials presents an attractive opportunity to leverage tunability in both organic and inorganic components.[11-13] PbS NCs have been interfaced with organic and inorganic materials for solar cells and photodetectors.[3,14-18] A previous study by Dissanayake *et al.* underscored the critical role of trap states at the PbS NC surface to describe photoelectron transfer.[19] A key aspect related to the integration of inorganic NCs with organic semiconductors is the understanding and control of electronic states at the NC surface. Performance in these devices has thus far fallen short of expectations based on an idealized band model picture of the heterojunction. Most likely this discrepancy can be explained by the presence of non-ideal states or trap states at the interface.

Current research on NC photovoltaics has identified several issues key to improving the power conversion efficiency.[20] Exciton dissociation at a NC interface has attracted attention, for understanding charge separation is crucial for optimizing optoelectronic devices.[21-23] However, low mobility in NC films has been a bottleneck towards high performance.[24] To address the low mobility, better understanding and control of charge trapping in NC films is required.[25] Charge trapping in NC films is a crucial issue for understanding the operation of optoelectronic NC devices. Particularly, NC trap states complicate the popular model of photogenerated exciton dissociation followed by carrier migration to the anode or cathode. Due to the high surface-to-volume ratio intrinsic to nanomaterials, NC surface states are suspected to modify the interfacial energy band alignment or create states within the NC band gap.[26] Sargent and co-workers recently demonstrated the reduction of trap states in hybrid (*i.e.,* organic and inorganic) surface passivation treatments via transient photovoltage measurements.[1] We studied electric field induced trapping by measuring the threshold voltage shift of a pentacene/PbS NC field effect transistor (FET) device. We created well-defined interface by thermal evaporation of pentacene onto a uniform thin film of NCs.

Figure 1 illustrates the device structure and the energy level alignment of PbS NCs relative to pentacene and the metal electrodes. PbS NCs were synthesized following the method of Hines *et. al.*,[27] (see supporting information). The NC diameter of 6.4 nm was calculated from the first exciton peak in the absorption spectrum at 1625 nm and confirmed by analysis of transmission electron micrographs as shown in the Supporting Information Figure S1.[28] We prepared uniform NC films of approximately one monolayer (~10 nm thickness) on pre-patterned FET electrodes using the doctor-blade method.[29] Details of the NC thin film coating are provided in Supporting Information (Figure S2). Prior to pentacene deposition, we modified the NC surface by exchanging the native oleic acid capping molecules for other surface ligands commonly used in NC devices. We exchanged the NC ligand by immersing NC films in a 0.1 M solution of the replacement ligand in acetonitrile or toluene for ethanedithiol (EDT) or other ligands respectively. The ligand exchange was performed in a nitrogen glovebox. A planar pentacene/PbS interface was formed by thermal deposition of pentacene molecules onto the PbS NC film at a pressure of 10^{-7} Torr and a rate of 0.2 nm/min.

Placement of PbS NCs between pentacene and the gate dielectric (300 nm SiO_2) alters the morphology of the pentacene film. The growth mode of pentacene is governed by the interactions of pentacene with other pentacene molecules and with the growth surface. As shown in Figure 2, pentacene exhibits a layered structure with a step height of ~1.5 nm corresponding to the thickness of a single molecular layer[30,31]. An atomic force microscopy (AFM) image of untreated (oleic acid capped) PbS NCs on SiO_2 is shown in Figure 2a featuring an *RMS* roughness of 0.3 nm. Mercaptopropionic acid (MPA) has been demonstrated as a common ligand replacement treatment to electronically couple proximate NCs in prototype photovoltaics[9,32]. The morphology of pentacene on MPA-treated PbS (Figure 2c) is similar pentacene on SiO_2 (Figure 2b) with a comparable grain size ranging between 100 and 200 nm. For pentacene deposited on NC films with dithiol ligands including ethaneditihol (EDT) (Figure 2d), biphenyl-4,4'-dithiol (BPDT) (Figure 2e) and 4,4'-dimercaptostilbene (DMS) (Figure 2f), the grain size is smaller than MPA-treated PbS, implying a higher nucleation density. Although the detailed nature of the interaction between pentacene and the ligands bound to the NC surface are not yet understood, we hypothesize that the size of the pentacene islands is related to the functional group (*i.e.* carboxylic acid *vs.* thiol) at the NC film surface.

Charge transport through the bilayer device must consider transport through the thick pentacene layer and the thinner NC film underneath. The AFM data of Figure 2 shows that the thickness of the pentacene layer is approximately 25 to 50 times that of the PbS NC layer. We point to several experimental indicators that suggests that conduction is dominated by the pentacene and not the PbS NCs. Supplementary figure S5 shows that the PbS NC monolayer is continuous as we were able to measure its transconductance and found it to be three orders of magnitude less than that of the PbS NC / pentacene bilayer (Figure 3(b)). This is also six orders of magnitude less than pentacene alone (Figure 3(a)). Despite this, we cannot exclude the possibility that conduction may occur by hopping between PbS NCs and pentacene. Whether or not the PbS NCs participate in conduction, the threshold voltage shifts we observe clearly show that charge trapping occurs when pentacene and PbS NCs form an interface.

We studied gate-field induced carrier trapping into the NC film by analyzing the threshold voltage. A change in the threshold voltage can be caused by a density of fixed charge (Q_{fc}) close to the conducting channel, according to $V_T=V_{fb}-(Q_{fc}/C_{ox})$, where V_{fb} is the flat-band voltage and C_{ox} is the capacitance of the SiO_2 gate dielectric. Change in the threshold voltage therefore provides a convenient measure of trapped charge.

Pentacene FETs without PbS NC showed near-zero threshold voltage (Figure 3a), which confirms that the control devices with neat pentacene films exhibit minimal charge trapping in the active layer.[31] In the forward (40 to -40 V) and reverse (-40 to 40 V) direction gate voltage sweeps, the threshold voltage difference is negligible due to insignificant charge trapping at the pentacene/SiO_2 interface. However, devices with an EDT-treated NC film between the pentacene and SiO_2 show threshold voltages during the forward and reverse voltage scans of 9 and -21 V, respectively (Figure 3b). The source-drain current in NC/pentacene bilayer devices is significantly reduced compared to the pentacene only device but still substantially higher than the NC only device. The threshold voltage is perturbed by the presence of charge carriers trapped at the NC-pentacene interface.

It has been shown that threshold voltage shift in pentacene FET devices can be caused by water adsorbed at the SiO_2-pentacene interface.[33] The devices studied in this paper were exposed to ambient air during transfer into the pentacene deposition chamber and during transfer into the vacuum chamber in which the measurements were performed. However, we believe the exposure to ambient to be a small effect relative to the effect of traps in the NC film. It has been shown that the effects on pentacene FETs by adsorbed water are reversible.[33,34] Therefore by measuring in vacuum we believe the effect of water was minimized. We demonstrate this by the transfer curve characteristics of the pentacene-only device in Figure 3. There is negligible threshold voltage shift relative to the device with NCs.

The magnitude of the shift in the threshold voltage, ΔV_{th}, during a forward gate scan can be correlated to the number of charge carriers, n, trapped per unit area as described by the relation: $n=(C_{ox}\Delta V_{th})/q$. The shift in the threshold voltage suggests that charges are trapped instead of contributing to conduction. As the electrical conductivity increases, the dielectric relaxation time τ_d, the characteristic time required to neutralize carriers decreases according to the relation $\tau_d=\rho\varepsilon_s$, where ρ is the resistivity and ε_s is the dielectric constant. A relaxation time in the PbS NCs longer than the time constant ($\sim 10^{-5}$ s) for the accumulation of holes in the pentacene channel is required to observe the threshold voltage shift arising from the built-in electric field. To meet this requirement, the electrical resistivity of the NC film should be larger than 10^8 (Ω cm). Indeed, we measured the resistivity of the PbS NC films to be greater than 10^8 (Ω cm) (see Supporting Figure S5).

To test an alternative hypothesis of the threshold voltage shift due to changing morphology of the pentacene film on the NCs, we created bilayer films with a thicker NC layer to move the heterogeneous interface away from the gate field. Pentacene deposited on a thick EDT-treated NC film showed a threshold voltage close to zero; this clarifies that the threshold voltage shift is associated with carrier trapping in NC films instead of the morphology of the pentacene film (see Supporting Figure S6).

To investigate the role of capping ligand on charge trapping, we used the ligand molecules shown in the inset of Figure 4. The I_D-V_G curves for four different capping molecules showed the most positive threshold voltage is observed in dimercaptostilbene (DMS) treated PbS NCs (see

Table I). The density of charges trapped, n, is estimated to be 10^{12} (cm^{-2}), or approximately 1 per NC.

We also investigated charge transfer of photogenerated carriers from pentacene to PbS NCs. Based on the absorption edge of pentacene (1.8 eV) we used a laser source of 650 nm wavelength (1.9 eV) to generate excitons in pentacene and NC film. The transfer curves (I_D vs. V_G) of Supporting Figure S3 show a positive threshold voltage shift and increased transconductance (dI_D/dV_G) under illumination. For the PbS NC/pentacene bilayer devices the positive threshold voltage shift under illumination may be due to accumulation of electrons in the pentacene as well as trapping of holes in the PbS NCs. Positive threshold voltage shift upon illumination has been demonstrated in pentacene only devices and is understood to be due to accumulation of minority carrier electrons[35,36]. However, the mobility of the majority carrier was not significantly altered in those reports. We observe significant change in mobility upon illumination according to $\mu=(dI_D/dV_G)L/(WC_{ox}V_D)$ where L and W are the length and width of the transistor, C_{ox} is the gate oxide capacitance and V_D is the drain voltage. We interpret this in terms of charge transfer from the pentacene layer to the PbS NC film. The valence/conduction states of a 6.4 nm PbS NC are about 4.25 eV and 5 eV below the vacuum level respectively[23]. The lowest unoccupied molecular orbital (LUMO) of pentacene is about 3 eV below the vacuum level[37]. Therefore any deep mid-gap states in the PbS NCs exist well below the photo-excited electron energy. Photogenerated excitons in the pentacene film close to the PbS NC layer could dissociate at the interface and transfer an electron to a trap state in the PbS NCs.

We studied field-induced carrier trapping by PbS NCs using a layered pentacene/PbS transistor. We quantified the number of charge carriers trapped by measuring the magnitude of the threshold voltage shift. Furthermore, we demonstrated that the ligand molecule alters the trap density. The approach detailed in this work provides a method to study surface traps or interface states crucial for understanding the performance of NC-based optoelectronic devices.

	Forward Sweep (V)	Reverse Sweep (V)	Total Shift (V)	Trapped Carrier Density (cm^{-2})	Trapped Carrier Density per NC
BPDT	9.2	-20	29.2	9.2x10^{11}	0.7
EDT	8.8	-21.4	30.2	8.8x10^{11}	0.7
DMS	13.6	-16.6	30.2	1.4x10^{12}	1.1
MPA	8.9	-19.8	28.7	8.9x10^{11}	0.7

Table I. Threshold voltage measurements calculated from the transfer curves of Figure 4.

ASSOCIATED CONTENT

Supporting Information. The supporting information details the nanocrystal optical absorption and TEM image describing the particle uniformity. The drag coating method is described. Photoinduced charge transfer at the Pentacene/PbS interface under light and dark conditions and charge transport of PbS only films are provided.

AUTHOR INFORMATION

Corresponding Author

Byoungnam Park (metalpbn@hongik.ac.kr) and Tobias Hanrath (th358@cornell.edu)

Present Address

B.P. Current Address: Department of Materials Science and Engineering Hongik University 72-
1, Sangsu-dong, Mapo-gu, Seoul 121-791 (Korea)

Author Contributions

B.P. and K.W. contributed equally.

Funding Sources

B.P. was supported by the Basic Energy Sciences Division of the Department of Energy through Grant DE-FG02-87ER45298. K.W. was supported partially from the Basic Energy Sciences Division of the Department of Energy Basic Energy Sciences Division through Grant DE-SC0006647 ‘Charge Transfer Across the Boundary of Photon-Harvesting Nanocrystals’ and partially from the NSF IGERT program (DGE-0654193).

Notes

Any additional relevant notes should be placed here.

ACKNOWLEDGMENT

This work made use of the Cornell Center for Materials Research Shared Facilities which are supported through the NSF MRSEC program (DMR-1120296). B.P. was supported by the Basic Energy Sciences Division of the Department of Energy through Grant DE-FG02-87ER45298. K.W. was supported partially from the Basic Energy Sciences Division of the Department of Energy Basic Energy Sciences Division through Grant **DE-SC0006647** ‘Charge Transfer Across the Boundary of Photon-Harvesting Nanocrystals’ and partially from the NSF IGERT program (DGE-0654193). This work was performed in part at the Cornell NanoScale Facility, a member of the National Nanotechnology Infrastructure Network, which is supported by the National Science Foundation (Grant ECCS-0335765).

REFERENCES

[1] A.H. Ip, S.M. Thon, S. Hoogland, O. Voznyy, D. Zhitomirsky, R. Debnath, L. Levina, L.R. Rollny, G.H. Carey, A. Fischer, K.W. Kemp, I.J. Kramer, Z. Ning, A.J. Labelle, K.W. Chou, A. Amassian, and E.H. Sargent, Nature Nanotechnology, **7**, 349 (2012).

[2] X. Wang, G.I. Koleilat, J. Tang, H. Liu, I.J. Kramer, R. Debnath, L. Brzozowski, D.A.R. Barkhouse, L. Levina, and S. Hoogland, **5**, 480 (2011).

[3] J.J. Choi, W.N. Wenger, R.S. Hoffman, Y.-F. Lim, J. Luria, J. Jasieniak, J.A. Marohn, and T. Hanrath, Adv. Mater. **23**, 3144 (2011).

[4] J.B. Sambur, T. Novet, and B.A. Parkinson, Science **330**, 63, (2010).

[5] O.E. Semonin, J.M. Luther, S. Choi, H.Y. Chen, J. Gao, A.J. Nozik, and M.C. Beard, Science **334**, 1530 (2011).

[6] W.A. Tisdale, K.J. Williams, B.A. Timp, D.J. Norris, E.S. Aydil, and X.Y. Zhu, Science **328**, 1543 (2010).

[7] J.J. Choi, Y.-F. Lim, M.B. Santiago-Berrios, M. Oh, B.-R. Hyun, L. Sun, A.C. Bartnik, A. Goedhart, G.G. Malliaras, H.D. Abruña, F.W. Wise, and T. Hanrath, Nano Lett. **9**, 3749 (2009).

[8] D.A.R. Barkhouse, R. Debnath, I.J. Kramer, D. Zhitomirsky, A.G. Pattantyus-Abraham, L. Levina, L. Etgar, M. Grätzel, and E.H. Sargent, Adv. Mater. **23**, 3134 (2011).

[9] A.G. Pattantyus-Abraham, I.J. Kramer, A.R. Barkhouse, X. Wang, G. Konstantatos, R. Debnath, L. Levina, I. Raabe, M.K. Nazeeruddin, M. Grätzel, and E.H. Sargent, ACS Nano **4**, 3374 (2010).

[10] L. Sun, J.J. Choi, D. Stachnik, A.C. Bartnik, B.-R. Hyun, G.G. Malliaras, T. Hanrath, and F.W. Wise, Nature Nanotechnology **7**, 369 (2012).

[11] P. Reiss, E. Couderc, J. De Girolamo, and A. Pron, Nanoscale **3**, 446 (2011).

[12] S. Ren, L.-Y. Chang, S.-K. Lim, J. Zhao, M. Smith, N. Zhao, V. Bulović, M. Bawendi, and S. Gradečak, Nano Lett. **11**, 3998 (2011).

[13] X. Jiang, R.D. Schaller, S.B. Lee, J.M. Pietryga, V.I. Klimov, and A.A. Zakhidov, J. Mater. Res. **22**, 2204 (2011).

[14] S. Cate, J.M. Schins, and L.D.A. Siebbeles, ACS Nano **6**, 8983 (2012).

[15] J. Tang, K.W. Kemp, S. Hoogland, K.S. Jeong, H. Liu, L. Levina, M. Furukawa, X. Wang, R. Debnath, D. Cha, K.W. Chou, A. Fischer, A. Amassian, J.B. Asbury, and E.H. Sargent, Nature Materials **10**, 765 (2011).

[16] N. Zhao, T.P. Osedach, L.-Y. Chang, S.M. Geyer, D. Wanger, M.T. Binda, A.C. Arango, M.G. Bawendi, and V. Bulović, ACS Nano **4**, 3743 (2010).

[17] V. Sukhovatkin, S. Hinds, L. Brzozowski, and E.H. Sargent, Science **324**, 1542 (2009).

[18] G. Konstantatos, I. Howard, A. Fischer, S. Hoogland, J. Clifford, E. Klem, L. Levina, and E.H. Sargent, Nature **442**, 180 (2006).

[19] D.M.N.M. Dissanayake, R.A. Hatton, T. Lutz, R.J. Curry, and S.R.P. Silva, Nanotechnology **20**, 195205 (2009).

[20] H.W. Hillhouse and M.C. Beard, Current Opinion in Colloid & Interface Science **14**, 245 (2009).

[21] S.M. Willis, C. Cheng, H.E. Assender, and A.A.R. Watt, Nano Lett. **12**, 1522 (2012).

[22] B. Ehrler, K.P. Musselman, M.L. Böhm, F.S.F. Morgenstern, Y. Vaynzof, B.J. Walker, J.L. MacManus-Driscoll, and N.C. Greenham, ACS Nano **7**, 4210 (2013).
[23] B.-R. Hyun, Y.-W. Zhong, A.C. Bartnik, L. Sun, H.D. Abruña, F.W. Wise, J.D. Goodreau, J.R. Matthews, T.M. Leslie, and N.F. Borrelli, ACS Nano **2**, 2206 (2008).
[24] Y. Liu, M. Gibbs, J. Puthussery, S. Gaik, R. Ihly, H.W. Hillhouse, and M. Law, Nano Lett. **10**, 1960 (2010).
[25] I.J. Kramer and E.H. Sargent, ACS Nano **5**, 8506 (2011).
[26] M. Soreni-Harari, N. Yaacobi-Gross, D. Steiner, A. Aharoni, U. Banin, O. Millo, and N. Tessler, Nano Lett. **8**, 678 (2008).
[27] M.A. Hines and G.D. Scholes, Adv. Mater. **15**, 1844 (2003).
[28] I. Moreels, Y. Justo, B. De Geyter, K. Haustraete, J.C. Martins, and Z. Hens, ACS Nano **5**, 2004 (2011).
[29] B.G. Prevo and O.D. Velev, Langmuir, **20**, 2099, (2004).
[30] D.J. Gundlach, Y.Y. Lin, T.N. Jackson, S.F. Nelson, and D.G. Schlom, IEEE Electron Device Lett. **18**, 87 (1997).
[31] D. Knipp, R.A. Street, A. Völkel, and J. Ho, J. Appl. Phys. **93**, 347 (2003).
[32] P.V. Kamat, J. Phys. Chem. C **115**, 13511 (2011).
[33] G. Gu, M.G. Kane, J.E. Doty, and A.H. Firester, Appl. Phys. Lett. **87**, 243512 (2005).
[34] G. Gu, M.G. Kane, and S.-C. Mau, J. Appl. Phys. **101**, 014504 (2007).
[35] Y.-Y. Noh and D.-Y. Kim, Solid-State Electronics **51**, 1052 (2007).
[36] Y. Liang, G. Dong, Y. Hu, L. Wang, and Y. Qiu, Appl. Phys. Lett. **86**, 132101 (2005).
[37] A. Kahn, N. Koch, and W. Gao, J. Polym. Sci. B Polym. Phys. **41**, 2529 (2003).
[38] Y. Wang, O. Acton, G. Ting, T. Weidner, P.J. Shamberge, H. Ma, F.S. Ohuchi, D.G. Castner, and A.K.Y. Jen, Organic Electronics **11**, 1066 (2010).
[39] D. Kumaki, M. Yahiro, Y. Inoue, and S. Tokito, Appl. Phys. Lett. **90**, 133511 (2007).

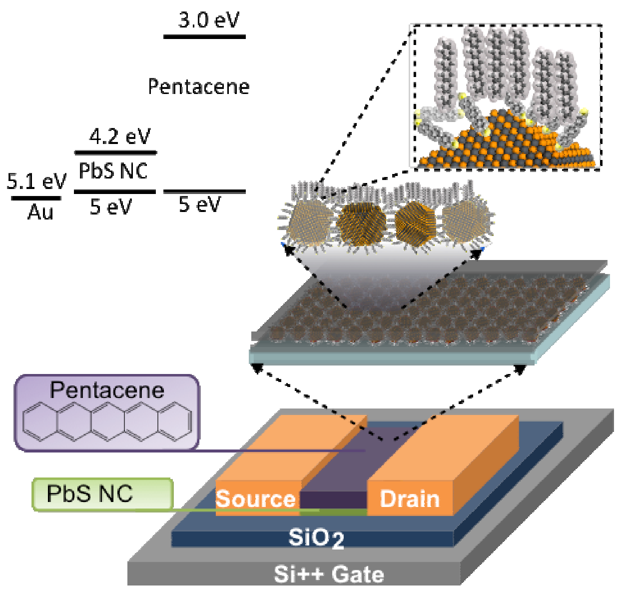

Figure 1. Schematic of a pentacene/PbS NC bilayer field effect transistor. The inset shows the structure of the pentacene/PbS NC interface and the energy level alignment.

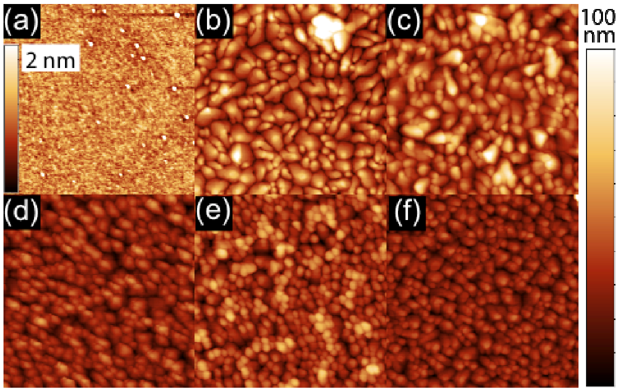

Figure 2. (a) AFM height image of untreated doctor-blade cast PbS NCs (RMS roughness, $R_q = 0.3$ nm). Pentacene grown on (b) SiO_2 (R_q = 16 nm), (c) MPA-treated PbS NCs (R_q = 15 nm), (d) EDT-treated PbS NCs (R_q = 9 nm), (e) BDT-treated PbS NCs (R_q = 12 nm), (f) DMS-treated PbS NCs (R_q = 8 nm). All images are 3 μm x 3 μm.

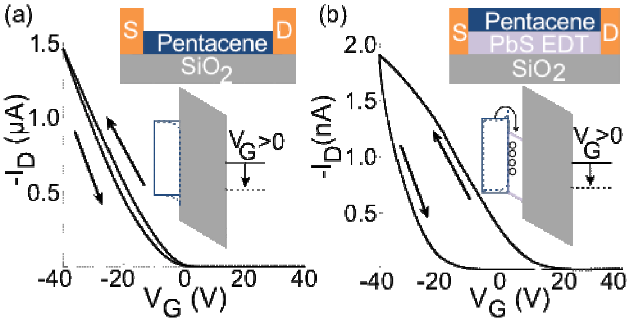

Figure 3. Transfer curves for (a) pentacene and (b) pentacene on EDT-treated PbS NCs. V_{SD} bias was -5 V. Channel length and width were 40 μm and 1 mm respectively. Insets show schematic structures and energy band diagrams. The energy band diagram in (a) shows carrier depletion in pentacene with positive gate bias. The band diagram in (b) shows accumulation of holes in pentacene due to transfer of electrons to trap sites at the interface with PbS NCs.

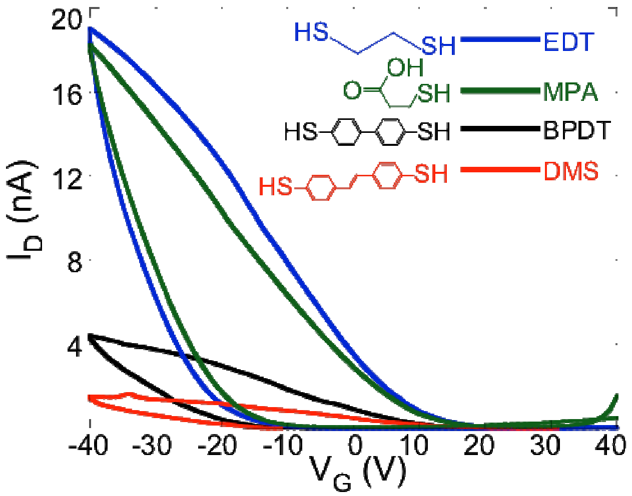

Figure 4. Transfer curves for FET devices with pentacene on a monolayer of PbS NCs treated with EDT, MPA, BPDT, and DMS ligands. Threshold voltages were calculated by linear interpolation of the forward and reverse segments of each curve. The transistor width and length were 1 mm and 40 µm, respectively.